Elsevier Editorial System(tm) for Journal of Colloid and Interface Science
Manuscript Draft

Manuscript Number: JCIS-17-2364

Title: The Zn and Pd Co-Modified TiO2 with Improved Photocatalytic Activity on Photo-Reduction of CO2 into CH4

Article Type: Full length article

Section/Category: A. Colloidal Materials and Nanomaterials

Keywords: Visible response; Surface Species; Photoreduction of CO2

Corresponding Author: Professor Yaan Cao,

Corresponding Author's Institution: Nankai University

First Author: Yanlong Yu

Order of Authors: Yanlong Yu; Limei Guo; Enjun Wang; Yaan Cao

Abstract: The Zn and Pd co-modified TiO2 photocatalyst exhibit remarkably enhanced photocatalytic activity on photo-reduction of CO2 with H2O into CH4. It is revealed that the introduced Zn and Pd exist as unique O-Zn-Cl and O-Pd-O species on the surface of TiO2, resulting in the enhanced absorption in visible region and efficient separated charge carriers. It can be deduced from the theory calculation and experiment results that the energy level of O-Zn-Cl and O-Pd-O match the redox potential, leading to the improvement of photocatalytic performance. These results suggest that the introduction of surface species is effective method to improve the photocatalytic activity, which can be applied in many fields.

Suggested Reviewers: Hong Liu
State Key Laboratory of Crystal Materials, Center of Bio & Micro/Nano Functional Materials, Shandong University
hongliu@sdu.edu.cn

Hua Chun Zeng
Department of Chemical and Biomolecular Engineering Facultyof Engineering National Universityof Singapore
chezhc@nus.edu.sg

Shinri Sato
Graduate School of Engineering Science, Osaka University
shinri@d7.dion.ne.jp

Michael Bowker
Department of Chemistry, Cardiff University
m.bowker@rdg.ac.uk

Hui-Ming Cheng
Chinese Academy of Sciences.
cheng@imr.ac.cn

Dear Editors:

We would like to submit the enclosed manuscript entitled “The Zn and Pd Co-Modified TiO_2 with Improved Photocatalytic Activity on Photo-Reduction of CO_2 into CH_4”. The Zn and Pd surface-modified TiO_2 photocatalyst exhibit remarkably enhanced photocatalytic activity on photo-reduction of CO_2 into CH_4. It can be deduced from the theory calculation and experiment results that the energy level of O-Zn-Cl and O-Pd-O match the redox potential, the absorption is enhanced significantly into visible region and the charge carriers are separated efficiently. We wish this work to be considered for publication in **Journal of Colloid and Interface Science**.

I would like to declare on behalf of my co-authors that the work described was original research that has not been published previously, and not under consideration for publication elsewhere, in whole or in part. We deeply appreciate your consideration of our manuscript, and we look forward to receiving comments from the reviewers. If you have any queries, please don’t hesitate to contact me at the address below.

Thank you and best regards.

Yours sincerely, Cao Yaan

Corresponding author: Name: Cao Yaan

E-mail: caoya@nankai.edu.cn

***3: Graphical Abstract**

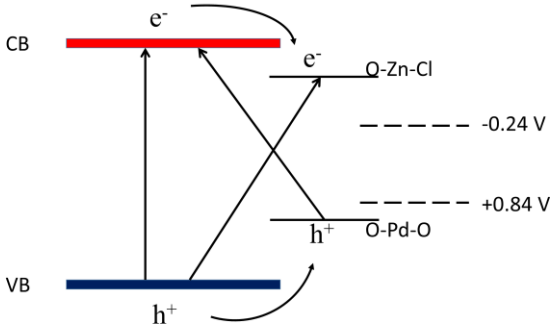

Schematic bans structure of TiO_2-Pd-Zn.

The Zn and Pd Co-Modified TiO_2 with Improved Photocatalytic Activity on Photo-Reduction of CO_2 into CH_4

Yanlong Yu[a,c], Limei Guo[a] , Enjun Wang[b],* and Yaan Cao[a]*

[a] MOE Key Laboratory of Weak-Light Nonlinear Photonics, Ministry of Education, TEDA Applied Physics Institute and School of Physics, Nankai University, Tianjin 300457, China

[b] Hefei Institutes of Physical Science, Chinese Academy of Sciences, Hefei 230031, China

[c] Department of Materials Chemistry, College of Chemistry, Nankai University, Tianjin 300457, China

ABSTRACT: The Zn and Pd co-modified TiO_2 photocatalyst exhibit remarkably enhanced photocatalytic activity on photo-reduction of CO_2 with H_2O into CH_4. It is revealed that the introduced Zn and Pd exist as unique O-Zn-Cl and O-Pd-O species on the surface of TiO_2, resulting in the enhanced absorption in visible region and efficient separated charge carriers. It can be deduced from the theory calculation and experiment results that the energy level of O-Zn-Cl and O-Pd-O match the redox potential, leading to the improvement of photocatalytic performance. These results suggest that the introduction of surface species is effective method to improve the photocatalytic activity, which can be applied in many fields.

KEYWORDS: Visible response; Surface Species; Photoreduction of CO2

Introduction

The photo-reduction of CO_2 into CH_4 via semiconductor photocatalysis has been investigated by many researchers since it applies solar light to convert CO_2 into valuable carbon fuels, methane[1-5]. The mechanism of photo-reduction CO_2 into CH_4 via photocatalysis can be described as follows[6-10]:

$$\text{Photocatalyst} + h\nu \rightarrow e^- + h^+ \quad (1)$$

$$2H_2O + 4h^+ \rightarrow O_2 + 4H^+ \quad E_o = 0.82V \text{ (vs NHE)} \quad (2)$$

$$CO_2 + 8e^- + 8H^+ \rightarrow CH_4 + 2H_2O \quad E_o = -0.24V \text{ (vs NHE)} \quad (3)$$

Under illumination, the photocatalysts are excited to generate electrons and holes in the conduction band and valence band, respectively (eqn 1). The photogenerated holes react with the adsorbed H_2O to form H^+ and oxygen (eqn 2, E_o= 0.82V (vs NHE)). Meanwhile, the exited electrons would be captured directly by the surface adsorbed CO_2 molecules to form CO and oxygen. The resultant CO would further react with electrons and H^+ to generate the final product, CH_4 (eqn 3, Eo= -0.24V (vs NHE)). Hence, it is necessary for the active photocatalyst that the energy level of conduction band and valence band should match the redox potential (eqn 2 and eqn 3) of photo-reduction of CO_2 into CH_4, the absorption should be extended into visible region effectively and the photogenerated charge carriers should be separated efficiently, enabling more electrons and holes participate in the photocatalytic reaction.

TiO_2 is one of the most promising photocatalysts on photoreduction of CO_2 into CH_4, due to its good performance and stability[6, 8, 11-13]. However, the photocatalytic efficiency of TiO_2 is still limited because of its large band gap (3.2 eV), rapid recombination of charge carrier, especially mismatch of redox potential for the photoreduction of CO_2 into CH_4. The modification with metal or nonmetal elements is considered as an effective method to enhance the visible response, separate the charge carriers as well as design and adjust the energy level of photocatalyst, so as to match the redox potential for the photoreduction of CO_2 into CH_4, leading to a full use of photogenerated charge carriers. Doping or modification with Pd[14-19] is usually regarded as quite an effective method to improve the photocatalytic performance of TiO_2 based catalyst. Recently, we have found out that TiO_2 modified with O-Pd-O surface species could show strong absorption in visible region and suppress the recombination of charge carriers efficiently[20-22], exhibit remarkable photocatalytic activity. In addition, the existence of unique O-Zn-Cl species on the surface of TiO_2 is also confirmed.[15] Based on discussion above, it is expected to introduce both O-Pd-O and O-Zn-Cl species into TiO_2 system to obtain a highly reactive photocatalyst on reduction of CO_2 into CH_4 for practical application.

In this work, the Pd and Zn co-modified TiO_2 samples were synthesized via a simple sol-gel method. The introduced Zn and Pd ions exist as unique O-Zn-Cl and O-Pd-O species on the surface of TiO_2. The band structure of TiO_2-Pd-Zn is investigated theoretically and experimentally. The behaviors of the photogenerated charge carriers are also investigated in details.

Experimental Details

Catalyst Preparation.

All chemicals used were of analytical grade and the water was deionized water (>18.2 MΩ•cm). At room temperature, different amounts of $PdCl_2$ solution and $Zn(NO_3)_2$ were dissolved into 40 mL of ethanol. After mixing for half an hour, 1 mL of HCl solution (12mol/L) and 12 mL of $Ti(OC_4H_9)_4$ was added dropwise into the mixture under vigous stirring. Then 1 mL of deionized water was added for further hydrolysis. The pH value of the mixture is evaluated to be 0.5. The mixture was stirred until the formation of TiO_2 gel. After aging for 24 hours, the TiO_2 gels were dried at 373K for 10 h and annealed at 723K in a muffle for 2.5h. The obtained samples were denoted as TiO_2-PdX-ZnY, where the X and Y stand for the nominal molar ratio of Zn^{2+} and Pd^{2+} to Ti^{4+} (Zn/Ti and Pd/Ti), respectively. Pure TiO_2, 5% of Zn modified TiO_2 (TiO_2-Zn) and 1.5% of Pd modified TiO_2 (TiO_2-Pd1.5%) were prepared using the same procedure without the addition of corresponding precursor.

Characterization.

Raman spectra were taken on a Renishaw in Via Raman microscope by using the 785 nm line of Renishaw HPNIR 785 semiconductor laser. X-Ray diffraction (XRD) patterns were acquired on a Rigaku D/max 2500 X-ray diffraction spectrometer (Cu Ka, λ=1.54056 Å) at a scan rate of 0.02° 2θ s^{-1}. The average crystal size was calculated using the Scherrer equation ($D=k\lambda/B\cos\theta$). After degassing at 180 °C, the BET surface area was determined via the measurement of nitrogen adsorption–desorption isotherms at 77 K (Micromeritics Automatic Surface Area Analyzer Gemini 2360, Shimadzu). X-Ray photoelectron spectroscopy (XPS) measurements were carried out with an ESCA Lab 220i-XL spectrometer by using an unmonochromated Al Ka X-ray source (148.6 eV). All spectra were calibrated using the binding energy (BE) of the adventitious C1s peak at 284.8 eV. Diffuse reflectance UV-vis absorption spectra (UV-Vis DRS) were collected with a UV-vis spectrometer (U-4100, Hitachi). Photoluminescence (PL) spectra were acquired by using the 325 nm line of a nano-second Nd:YAG laser (NL303G) as excitation source. The experimental setup consists of a spectrometer (Spex 1702), a photomultiplier tube (PMT, Hamamatsu R943), a lock-in amplifier, and a computer for data processing. All

of the measurements were carried out at room temperature (25±2 °C). The surface photovoltage spectroscopy (SPS) was measured on a solid-junction photovoltaic cell of indium tin oxide (ITO)/sample/ITO equipped with a lock-in amplifier (Model SR830, DSP) and synchronized with a light chopper. The monochromatic light was obtained by passing light from a 500W xenon lamp (CHF-XQ 500W) through a double prism monochromator (WDG30-2).

Evaluation of Photocatalytic Activity.

The photo-reduction activity of the photocatalysts was evaluated by photo-reduction of CO_2 and H_2O into CH4. 150 mg of photocatalyst was uniformly dispersed on a glass sheet with an area of 9.4 cm^2. A 500 W spherical Xenon arc lamp (Philips, Belgium, 35mW/cm^2, 290 nm ~ 800 nm) was used as the light source of photocatalytic reaction. The glass sheet was placed at the bottom of a sealed Pyrex glass reaction vessel (410 mL) which is located 10 cm away from the light source and vertical to the light beam. Prior to the illumination, the high purity of CO_2 gas (99.99%), via a flow controller, was followed into the reaction setup for 45 min for reaching ambient pressure. Then the reaction vessel was sealed and 2 mL of deionized water was injected into the reaction system as reducer. During irradiation, about 0.4 mL of gas was continually taken from the reaction cell every 2 h for subsequent CH_4 and CO concentration analysis by using a gas chromatograph (Techcomp GC-7890F, equipped with a 1 m×3 mm TDX-01 packed column and a flame ionization detector (FID)]. N_2 was used as the carrier gas. Since FID cannot detect CO and CO_2, an additional converter (Techcomp converter loaded with Ni catalyst) was attached to the GC system between the column and detector, which can reduce CO to methanol ($CO + H_2 \rightarrow CH_3OH$) and CO_2 to methane ($CO_2 + 4H_2 \rightarrow CH_4 + 2H_2O$). Hence, CO and CO_2 could be analysed simultaneously. The relative humidity and temperature in the reactor during the photosynthesis process is maintained as 80% and 30^oC.

DFT Calculation

The calculations were carried out by a first-principle calculation software package CASTEP. Generalized gradient approximation (GGA) based density-functional theory (DFT) was used to calculate the electronic band structure and density of states (DOS) for pure TiO_2, TiO_2-Zn and TiO_2-Pd, respectively. An anatase TiO_2 model of 76 atoms with exposed (101) facet is created. The vacuum lamb is set as 10 Ai. For TiO_2-Pd, one Pd ion is linked with two surface bridge O ions on the (101) facet. For TiO_2-Zn, one Zn ion is linked with one surface bridge O ion on the (101) surface of anatase and one Cl ion. The valence electronic configurations for O, Ti, Cl, Zn and Pd atoms were $2s^22p^4$, $3s^23p^63d^24s^2$, $3s^23p^5$, $3d^{10}4s^2$ and $4d^{10}$, respectively. The plane wave energy cutoffs were taken to be 420 eV. In all the cases, geometry optimizations were carried out first, and convergence was assumed when the forces on atoms were less than 50 meV/Å. Compared with experimental results, the theoretical calculation usually re-

sults in an underestimated band gap, caused by the shortcoming of the exchange-correction functional in describing the excited states[23, 24].

Results and Discussion

To investigate the band structure of TiO_2 modified with O-Pd-O and O-Zn-Cl species, theoretical calculation based on density functional theory are carried out for TiO_2-Pd and TiO_2-Zn, as shown in Figure 1. The theory calculation results of pure TiO_2 are plotted in Figure S8. The zero point suggests the highest occupied energy level of the valence band. The conduction band of TiO_2 mainly consist of Ti 3d and a small fraction of O 2p orbitals, and the valence band is composed of O 2p with a small fraction of Ti 3d orbitals. For TiO_2-Zn samples, a new doping energy level corresponding to O-Zn-Cl species occurred below the conduction band of TiO_2. The new energy level mainly consists of Zn 4s and Cl 3p orbitals. For the TiO_2-Pd samples, new energy levels of O-Pd-O species on the surface of TiO_2 occurred above the valence band of TiO_2. The energy bands are composed of Pd 4d orbitals, hybridized with O 2p and Ti 3d states. These calculated results imply that the introduction of O-Pd-O and O-Zn-Cl species makes the band structure of photocatalyst match the redox potential of photo-reduction of CO_2 into CH_4 more compatible. It is expected that the absorption of TiO2-PdX-ZnY would be extend into visible region, leading to an improved photocatalytic activity on photo-reduction of CO_2 into CH_4.

To investigate the crystal structure of the obtained samples, the Raman patterns of the TiO_2, TiO_2-Pd, TiO_2-Zn and TiO_2-Pd1.5%-Zn5% samples are shown in Figure 2. All samples show the typical characteristic bands at about 142 cm^{-1}, 195 cm^{-1}, 395 cm^{-1}, 515 cm^{-1} and 637 cm^{-1}, attributed to the Eg, B1g, A1g, B2g and Eg vibrational modes of anatase[25], respectively. For TiO_2-PdX-ZnY with different amount of Zn and Pd (Figure S1), all the samples remain anatase structure. The peak position of Raman peaks is almost unchanged, indicating both Pd and Zn ions didn't enter into TiO_2 lattice and may exist on the surface of TiO_2. In addition, two additional weak Raman peaks at about 256 cm^{-1} and 333 cm^{-1} are observed for the Zn modified TiO_2 as well as the Pd and Zn co-modified TiO_2 samples (Figure S1). These two peaks are ascribed to stretching modes of Zn-Cl and Zn-O bonds, respectively, suggesting the existence of O-Zn-Cl species on TiO_2 surface. The XRD patterns of the TiO_2, TiO_2-Pd, TiO_2-Zn and TiO_2-PdX-ZnY samples are shown in Figure S2. It is clear that all samples exhibit typical anatase structure and there is no other phase, such as rutile, ZnO, $ZnTiO_3$ and PdO, observed in the XRD patterns. It is noted that $ZnTiO_3$ will occur when the molar ratio of Zn/Ti is above 10%.[15] The lattice parameters, cell volumes and crystal size are calculated and summarized in Table S2 from the XRD patterns. No shift for the diffraction peaks is observed (Figure S2) and the lattice parameters as well as the cell volume almost remain the same for the TiO_2-Pd, TiO_2-Zn and TiO_2-PdX-ZnY samples, compared with pure

TiO_2 (Table S1). Therefore, it becomes reasonable to deduce that neither Pd^{2+} ions nor Zn^{2+} ions are doped into TiO_2 lattice. The introduced Pd^{2+} ions and Zn^{2+} ions may exist as some kinds of species on the surface of TiO_2. Furthermore, after the introduction of Pd and Zn, the BET specific surface areas increase in the order of TiO_2 < TiO_2-Zn < $TiO_{0.}$-Pd < TiO2-Pd-Zn. The crystallite sizes decrease in the order of TiO2-Pd-Zn < TiO2-Zn < TiO2-Pd < TiO2. The detailed existing states of Pd and Zn are investigated by XPS in the following sections.

Figure 3A shows XPS Cl 2p spectra of TiO_2, TiO_2-Pd, TiO_2-Zn and TiO_2-Pd-Zn. The peak centered at about 198.1 eV for TiO_2 and TiO_2-Pd is ascribed to Cl 2p of the O-Ti-Cl species on the surface of TiO_2. It has been demonstrated by our previous work that the Cl^- ions link with the surface unsaturated Ti sites to form the O-Ti-Cl species which shows no visible response and hardly influence the photocatalytic activity[22, 26, 27]. In comparison with pure TiO^2, the peak intensity of Cl 2p for TiO_2-Pd remains unchanged, suggesting no other Cl species is formed on the surface of TiO_2. For the TiO_2-Zn and TiO_2-Pd1.5%-Zn5% samples, the peak intensity of the Cl 2p increase significantly, centered at about 198.9 eV and 198.7 eV, respectively, locating between that of $TiCl_4$ (198.2 eV) and $ZnCl_2$ (199.7 eV)[9]. Moreover, compared with TiO_2 (2.01%) and TiO_2-Pd (2.36%), the atom percentage calculated from the XPS also increases remarkably for TiO_2-Zn (6.49%) and TiO_2-Pd-Zn(5.25%). This suggests that the Cl- ions may links with only Zn^{2+} ions to form Zn-Cl bonds on the surface of TiO_2. Moreover, as shown in Figure 3B, the center of the Zn $2p_{3/2}$ peak for the Zn 2p spectra of TiO_2-Zn (1022.1 eV) and TiO_2-Pd-Zn (1022.0 eV) locates between that of ZnO (1021.5 eV)[28] and $ZnCl_2$ (1022.5 eV)[29], indicating one Zn^{2+} ion link with one unsaturated O atom and one Cl^- ion to exist as O-Zn-Cl species[29, 30]. For the Pd 3d spectra (Figure 3C), the peaks of Pd $3d_{5/2}$ for TiO_2-Pd and TiO_2-Pd-Zn locate at about 336.7 eV, attributed to the O-Pd-O structure on the surface of TiO_2 (one Pd^{2+} ions linked with two unsaturated O^{2-} ions)[31, 32]. Hence, it is concluded that the introduced Pd ions exist as O-Pd-O species and the introduced Zn ions exist as O-Zn-Cl species on the surface of TiO_2. These XPS results are in good agreement with the Raman and XRD results above.

The XPS valence band spectra, absorption spectra, photoluminescence (PL) spectra, time resolved PL and surface photovoltaic spectra (SPS) are carried out to investigate the band structure, visible response, separation and recombination behavior of charge carriers of the photocatalysts, which is closely related to the photocatalytic activity, as shown in Figure 4. XPS valence band spectra are plotted in Figure 4A. The energy scale for all samples are aligned by applying the work function of XPS instrument (4.1 eV, Fermi level)[33]. The binding energy of the onset edge for O 2p revealed the energy gap between the valence band top and the Fermi level (E_f). The valence band top for pure TiO_2 is estimated to be at about +2.7 eV (+2.3 V, vs NHE). Compared with pure TiO_2, the onset edge for TiO_2-Zn almost remained un-

changed. Furthermore, it is noted that a new energy level occurred at about +2.1 eV (+1.7V, vs NHE) for TiO_2-Pd and TiO_2-Pd-Zn, which is caused by the introduced Pd 4d orbitals corresponding to the O-Pd-O surface species. These results implied the introduction of O-Pd-O may promote the separation of charge carriers and increase the absorption in visible region. These XPS results are in good agreement with the theoretical calculation results.

The diffuse reflectance UV–visible absorption spectra of all samples are plotted in Figure 4B. TiO_2 shows strong absorption in UV region caused by the band to band transition. The onset edge is about 400 nm, corresponding to the band gap of 3.1 eV for TiO_2. The TiO_2-Zn shows weak threshold absorption from 400 nm to 600 nm, caused by the electron transition from the valence band to the surface energy level of O-Zn-Cl species. The position of the absorption maximum is at about 450 nm, indicating the surface energy level of O-Zn-Cl locates at 0.35 eV (-0.45V, vs NHE) below the conduction band (-0.8V, vs NHE). The absorption in visible region is enhanced significantly for TiO_2-Pd, owing to the surface O-Pd-O species[27]. It is found from the theoretical calculation and the XPS valence band spectra that the energy level of O-Pd-O species locates at about 0.6 eV above the valence band of TiO_2. Hence the absorption in visible region is ascribed to the electron transition from the energy levels of O-Pd-O species to the conduction band of TiO_2. Moreover, as we expect, the TiO_2-PdX-ZnY represent the strongest absorption in visible region (Figure S3), and with the increase of Pd or Zn content, the absorption in visible region is further improved, owing to synergistic effect of introduced O-Pd-O and O-Zn-Cl species. The band structure of TiO_2-PdX-ZnY samples are determined and drawn in Figure 6. As the energy level of O-Zn-Cl (-0.45 eV, vs NHE) and O-Pd-O (+1.7 eV, vs NHE) locate above and below the redox potential of reaction (3) (-0.24 V, vs NHE) and reaction (2) (+0.8V, vs NHE) respectively, the separated electrons and holes in the surface energy level are able to take part in the photocatalytic reaction on reduction of CO_2 into CH_4.

As shown in Figure 4C and S4, SPS reveals the separation behavior of photogenerated charge carriers, under irradiation from 300 nm to 800 nm. The higher peak intensity usually indicates the more efficient separation of charge carriers. The TiO_2-PdX-ZnY samples exhibit the highest visible light surface photovoltaic spectroscopic (SPS) response in the visible region (from 400 nm to 800 nm). At the same time, the TiO_2-Zn and TiO_2-Pd exhibit poor SPS response and pure TiO_2 almost shows no SPS response in visible region. These SPS results suggest that the more electrons and holes are generated and separated effectively for TiO_2-PdX-ZnY samples with the increase of Zn or Pd than TiO_2-Zn and TiO_2-Pd samples under visible irradiation.

For photocatalyst, the photogenerated electrons in the conduction band would fall into the oxygen vacancies through a nonirradiative process (τ1) and recombine with the holes via an irradiative process (τ2), leading to the emission of fluorescence. Hence, the quench of the photoluminescence (PL) spectra and prolonged life-time of charge carriers indicates efficient suppression of the recombination for photoinduced charge carriers. Figure 4D shows the PL spectra of TiO_2, TiO_2-Zn, TiO_2-Pd and TiO_2-Pd1.5%-Zn5%. It can be easily seen that the emission intensity of TiO_2-Zn is weakened compared with pure TiO_2, as the electrons could transfer into the surface energy level of O-Zn-Cl species. For TiO_2-Pd, the PL intensity is quenched significantly because the electrons and holes could transfer to the energy level of the O-Pd-O species. And the PL emission for TiO_2-PdX-ZnY is further quenched with the increase of Zn or Pd owing to the contribution from both the O-Zn-Cl and O-Pd-O species (Figure S5). Moreover, the τ1 and τ2 values related to the nonirradiative and irradiative process are shown in Table 1. The τ2 value for TiO_2-Zn and TiO_2-Pd is longer than that for TiO_2, as the electrons in the conduction band of TiO_2 could transfer to the energy level of O-Zn-Cl species or the holes in the valence band could move to the energy level of O-Pd-O species. For the TiO_2-Pd1.5%-Zn5% samples, the τ2 value is longer than the TiO_2-Zn and TiO_2-Pd due to the co-existence of O-Pd-O and O-Zn-Cl species. These photoluminescence (PL) spectra and time resolved PL decay time results suggest that the photogenerated electrons and holes are separated more efficiently for the Zn and Pd co-modified TiO_2 samples than TiO_2-Zn and TiO_2-Pd.

According to the discussion above, owing to the introduction of O-Pd-O and O-Zn-Cl species on the surface of TiO2 which might behave as “reactive sites”, the visible response is improved significantly and the charge carriers are separated efficiently, more photogenerated electrons and holes could participate in the photocatalytic reaction, suggesting a higher photocatalytic activity for TiO_2-PdX-ZnY than TiO_2-Pd and TiO_2-Zn.

The photo-reduction of CO_2 into CH_4 in the presence of water vapor under Xe lamp irradiation is applied to evaluate the photocatalytic activity of the obtained TiO_2-based photocatalysts. The photocatalytic experiment results are presented in Figure 5 and Table 2. The commercial available TiO_2 (Degussa P25) is also applied for comparison. In this experiment, CO is the intermediate product and CH4 is the final product. There is no other gas product detected, such as H_2, CH_3OH. After 8 hours’ irradiation, only 0.350 μmol and 0.358 μmol of CH_4 is detected in the presence of self-made pure TiO_2 sample and commercial TiO_2 (Degussa P25). The Zn modified TiO_2 sample (TiO_2-Zn) exhibit a limited photocatalytic activity and about 0.851 μmol of CH_4 is produced. After the modification with Pd, the photocatalytic performance of TiO_2-Pd is enhanced effectively and 3.59 μmol of CH_4 is generated. After the introduction of Zn and Pd into TiO_2, TiO_2-PdX-ZnY samples exhibit much better photocatalytic ac-

tivity than TiO_2-Zn and TiO_2-Pd on photo-reduction of CO_2 into CH_4. It is found TiO2-Pd1.5%-Zn5% sample exhibit the best photocatalytic activity among all photocatalysts and about 7.99 μmol of CH_4 is detected after 8 hours' irradiation, whose specific photocatalytic activity is almost twice as that for TiO_2-Pd and twenty times higher than that for P25. In addition, it is found from the XPS that the amount of C before and after the photocatalytic reaction is 15.34% and 18.63%, respectively, suggesting the surface absorbed carbon in the photocatalyst itself did not react with CO_2 to generate CO.

According to the discussion above, the enhancement of the photocatalytic mechanism could be explained with the assistance of schematic diagram band structure of TiO_2-PdX-ZnY, shown in Figure 6. Under irradiation, an electron is excited from the valence band to the conduction band, leaving a hole in the valence band. One electron migrate to the surface to active the CO_2 to form CO_2^-, which would further react with electron, proton, or hydrogen radical via a series of steps to break the C-O bonds and create C-H bonds.[1] In addition, it is also noted that some of the products could react with each other in an opposite way or be photo-absorbed.[34, 35] Pure TiO_2 photocatalyst shows poor visible response, the recombination rate of charge carriers are relatively high, and the position of conduction band and valence band are far from the redox potential (Figure 6), resulting in a poor photocatalytic activity on reduction of CO_2 into CH_4. For TiO_2-Zn, electrons can be excited from the valence band of TiO_2 to the surface energy level of O-Zn-Cl directly, and the electrons on the conduction band of TiO_2 would transfer to energy level of O-Zn-Cl species, to participate in the photocatalytic reaction. So, the TiO_2-Zn sample represents a higher photocatalytic activity than pure TiO_2. For TiO_2-Pd sample, the electrons can be excited from the energy level of O-Pd-O species to the conduction band of TiO_2. The holes in the valence band could also move to the energy level of O-Pd-O surface species. The electrons in the conduction band of TiO_2 and holes in the energy level of O-Pd-O species participate in the photocatalytic reaction. The TiO_2-Pd sample exhibit an enhanced photocatalytic activity compared with TiO_2 and TiO_2-Zn. Moreover, for TiO_2-PdX-ZnY samples, owing to the synergetic effect of surface O-Zn-Cl and O-Pd-O species, the visible response is further improved and charge carriers are separated efficiently. The O-Zn-Cl and O-Pd-O species would react as reactive sites, as their energy levels are below the conduction band and above the valence band, respectively. Photogenerated electrons and holes would first migrate to the surface of TiO_2 and be enriched in these surface reactive sites, which further take part in the photocatalytic reaction. Therefore, TiO_2-PdX-ZnY samples exhibit much better photocatalytic activity than the TiO_2-Zn and TiO_2-Pd samples.

Conclusions

Based on the theory calculation, a highly reactive photocatalyst, TiO_2-PdX-ZnY, is synthesized and exhibits significantly improved photocatalytic activity on reduction of CO_2 into CH_4. Owing to the existence of O-Zn-Cl and O-Pd-O surface species, the visible response is enhanced significantly and the charge carriers are separated effectively. As the energy level of O-Zn-Cl and O-Pd-O surface species is closely next to the redox potential of photo-reduction, more electrons and holes are enriched in the reactive sites (O-Zn-Cl and O-Pd-O surface species) and participate in the photocatalytic reaction, leading to remarkable improved photocatalytic activity for TiO_2-PdX-ZnY on photo-reduciton of CO2 into CH4.

Acknowledgements

This work was supported by National Natural Science Foundation of China (no. 51372120 and 51302269) and China Postdoctoral Science Foundation (no. 2017M611149). We thank Prof. Ying Ma from Institute of Chemistry, Chinese Academy of Sciences, and Prof. Yihong Ding from State Key Lab of Theoretical and Computational Chemistry, Jilin University for helping us to carry out the theoretical calculation.

ASSOCIATED CONTENT

Supporting Information. "This material is available free of charge via the Internet at http://pubs.acs.org."

AUTHOR INFORMATION

Corresponding Author

* Y.C. email address: caoya@nankai.edu.cn; E.W. email address: enjunwang@gmail.com

ACKNOWLEDGMENT

This work was supported by National Natural Science Foundation of China (no. 51372120 and 51302269) and China Postdoctoral Science Foundation (no. 2017M611149). We thank Prof. Ying Ma from Institute of Chemistry, Chinese Academy of Sciences, and Prof. Yihong Ding from State Key Lab of Theoretical and Computational Chemistry, Jilin University for helping us to carry out the theoretical calculation.

REFERENCES

[1] S.N. Habisreutinger, L. Schmidt-Mende, J.K. Stolarczyk, Photocatalytic Reduction of CO2 on TiO2 and Other Semiconductors, Angew. Chem. Int. Ed., 52 (2013) 7372-7408.

[2] K.F. Li, X.Q. An, K.H. Park, M. Khraisheh, J.W. Tang, A Critical Review of CO2 Photoconversion: Catalysts and Reactors, Catal. Today, 224 (2014) 3-12.

[3] L. Yuan, Y.J. Xu, Photocatalytic Conversion of CO2 into Value-Added and Renewable Fuels, Appl. Surf. Sci., 342 (2015) 154-167.
[4] O. Ola, M.M. Maroto-Valer, Review of Material Design and Reactor Engineering on TiO2 Photocatalysis for CO2 Reduction, J. Photochem. Photobiol. C Photochem. Rev., 24 (2015) 16-42.
[5] S. Bai, W. Yin, L. Wang, Z. Li, Y. Xiong, Surface and interface design in cocatalysts for photocatalytic water splitting and CO2 reduction, RSC Adv., 6 (2016) S7446-S7463.
[6] N.M. Dimitrijevic, B.K. Vijayan, O.G. Poluektov, T. Rajh, K.A. Gray, H. He, P. Zapol, Role of Water and Carbonates in Photocatalytic Transformation of CO2 to CH4 on Titania, J. Am. Chem. Soc., 133 (2011) 3964-3971.
[7] Q. Liu, Y. Zhou, Z. Tian, X. Chen, J. Gao, Z. Zou, Zn_2GeO_4 Crystal Splitting Toward Sheaf-like, Hyperbranched Nanostructures and Photocatalytic Reduction of CO_2 into CH_4 under Visible Light after Nitridation, J. Mater. Chem., 22 (2012) 2033-2038.
[8] S. Xie, Y. Wang, Q. Zhang, W. Fan, W. Deng, Y. Wang, Photocatalytic Reduction of CO_2 with H_2O: Significant Enhancement of the Activity of Pt–TiO_2 in CH_4 Formation by Addition of MgO, Chem. Commun. (Camb.), 49 (2013) 2451-2453.
[9] Y. Yan, Y. Yu, D. Wu, Y. Yang, Y. Cao, TiO2/vanadate (Sr10V6O25, Ni3V2O8, Zn2V2O7) heterostructured photocatalysts with enhanced photocatalytic activity for photoreduction of CO2 into CH4, Nanoscale, 8 (2015) 949-958.
[10] Y. Yu, L. Guo, H. Cao, Y. Lv, E. Wang, Y. Cao, A new Ni/Ni3(BO3)2/NiO heterostructured photocatalyst with efficient reduction of CO2 into CH4, Sep. Purif. Technol., 142 (2015) 14-17.
[11] K. Bhattacharyya, A. Danon, B. K. Vijayan, K.A. Gray, P.C. Stair, E. Weitz, Role of the Surface Lewis Acid and Base Sites in the Adsorption of CO_2 on Titania Nanotubes and Platinized Titania Nanotubes: An in Situ FT-IR Study, J. Phys. Chem. C, 117 (2013) 12661-12678.
[12] V.V. Galvita, H. Poelman, C. Detavernier, G.B. Marin, Catalyst-assisted chemical looping for CO2 conversion to CO, Applied Catalysis B-Environmental, 164 (2015) 184-191.
[13] C. Wang, R.L. Thompson, J. Baltrus, C. Matranga, Visible Light Photoreduction of CO_2 Using CdSe/Pt/TiO_2 Heterostructured Catalysts, The Journal of Physical Chemistry Letters, 1 (2009) 48-53.
[14] M. Bowker, D. James, P. Stone, R. Bennett, N. Perkins, L. Millard, J. Greaves, A. Dickinson, Catalysis at the Metal-Support Interface: Exemplified by the Photocatalytic Reforming of Methanol on Pd/TiO_2, J. Catal., 217 (2003) 427-433.
[15] Y. Yu, J. Wang, W. Li, W. Zheng, Y. Cao, Doping Mechanism of Zn2+ Ions in Zn-Doped TiO2 Prepared by a Sol–gel Method, CrystEngComm, 17 (2015) 5074-5080.
[16] F.N. Sayed, O. Jayakumar, R. Sasikala, R. Kadam, S.R. Bharadwaj, L. Kienle, U. Schürmann, S.r. Kaps, R. Adelung, J. Mittal, Photochemical Hydrogen Generation Using Nitrogen-Doped TiO2–Pd Nanoparticles: Facile Synthesis and Effect of Ti3+ Incorporation, J. Phys. Chem. C, 116 (2012) 12462-12467.
[17] A.T. Kuvarega, R.W.M. Krause, B.B. Mamba, Nitrogen/Palladium-Codoped TiO2for Efficient Visible Light Photocatalytic Dye Degradation, J. Phys. Chem. C, 115 (2011) 22110-22120.
[18] Q. Li, Y.W. Li, P. Wu, R. Xie, J.K. Shang, Palladium Oxide Nanoparticles on Nitrogen-Doped Titanium Oxide: Accelerated Photocatalytic Disinfection and Post-Illumination Catalytic "Memory", Adv. Mater., 20 (2008) 3717-3723.
[19] Q. Li, R. Xie, E.A. Mintz, J.K. Shang, Enhanced Visible-Light Photocatalytic Degradation of Humic Acid by Palladium-Modified Nitrogen-Doped Titanium Oxide, J. Am. Ceram. Soc., 90 (2007) 3863-3868.
[20] Y. Yu, E. Wang, J. Yuan, Y. Cao, Enhanced Photocatalytic Activity of Titania with Unique Surface Indium and Boron Species, Appl. Surf. Sci., 273 (2013) 638-644.
[21] Y. Cao, T. He, L. Zhao, E. Wang, W. Yang, Y. Cao, Structure and Phase Transition Behavior of Sn^{4+}-Doped TiO_2 Nanoparticles, J. Phys. Chem. C, 113 (2009) 18121-18124.
[22] Y. Cao, Y. Yu, P. Zhang, L. Zhang, T. He, Y. Cao, An Enhanced Visible-Light Photocatalytic Activity of TiO_2 by Nitrogen and Nickel–Chlorine Modification, Sep. Purif. Technol., 104 (2013) 256-262.

[23] W.L. Huang, Q. Zhu, Electronic structures of relaxed BiOX (X=F, Cl, Br, I) photocatalysts, Computational Materials Science, 43 (2008) 1101-1108.
[24] D. Zhao, X. Huang, B. Tian, S. Zhou, Y. Li, Z. Du, The effect of electronegative difference on the electronic structure and visible light photocatalytic activity of N-doped anatase TiO[sub 2] by first-principles calculations, Appl. Phys. Lett., 98 (2011) 162107.
[25] J. Wang, Y. Yu, S. Li, L. Guo, E. Wang, Y. Cao, Doping Behavior of Zr^{4+} Ions in Zr^{4+}-Doped TiO_2 Nanoparticles, J. Phys. Chem. C, 117 (2013) 27120-27126.
[26] E. Wang, W. Yang, Y. Cao, Unique Surface Chemical Species on Indium Doped TiO_2 and Their Effect on the Visible Light Photocatalytic Activity, J. Phys. Chem. C, 113 (2009) 20912-20917.
[27] D. Zhao, Y. Yu, C. Cao, J. Wang, E. Wang, Y. Cao, The existing states of doped B3+ ions on the B doped TiO2, Appl. Surf. Sci., 345 (2015) 67-71.
[28] W. Li, D. Wu, Y. Yu, P. Zhang, J. Yuan, Y. Cao, Y. Cao, J. Xu, Investigation on a novel ZnO/TiO2–B photocatalyst with enhanced visible photocatalytic activity, Physica E: Low-dimensional Systems and Nanostructures, 58 (2014) 118-123.
[29] Y. Yu, Y. Gu, W. Zheng, Y. Ding, Y. Cao, New Type Photocatalyst PbBiO 2 Cl: Materials Design and Experimental Validation, J. Phys. Chem. C, 119 (2015) 28190-28193.
[30] S. Yan, Y. Yu, Y. Gu, Y. Liu, Y. Cao, Improved photocatalytic activity of TiO 2 modified with unique O–Zn–Cl surface species, Sep. Purif. Technol., 171 (2016) 118-122.
[31] Y. Yan, Y. Yu, S. Huang, Y. Yang, X. Yang, S. Yin, Y. Cao, Adjustment and Matching of Energy Band of TiO2-Based Photocatalysts by Metal Ions (Pd, Cu, Mn) for Photoreduction of CO2 into CH4, J. Phys. Chem. C, (2017) 1089-1098.
[32] Y. Yu, T. He, L. Guo, Y. Yang, L. Guo, Y. Tang, Y. Cao, Efficient Visible-light Photocatalytic Degradation System Assisted by Conventional Pd Catalysis, Sci. Rep., 5:9561 (2015) 1-6.
[33] Y. Cao, T. He, Y. Chen, Y. Cao, Fabrication of Rutile TiO_2−Sn/Anatase TiO_2−N Heterostructure and Its Application in Visible-Light Photocatalysis, J. Phys. Chem. C, 114 (2010) 3627-3633.
[34] K. Koci, L. Obalova, O. Solcova, Kinetic Study of Photocatalytic Reduction of CO2 Over TiO2, Chemical and Process Engineering-Inzynieria Chemiczna I Procesowa, 31 (2010) 395-407.
[35] S.T. Seng, L. Zou, E. Hu, Kinetic Modelling for Photosynthesis of Hydrogen and Methane Through Catalytic Reduction of Carbon Dioxide with Water Vapour, Catal. Today, 131 (2008) 125-129.

Figure 1. Theoretical calculated band structure and Projected density of states (PDOS) for the TiO_2-Zn (A and B) and TiO_2-Pd (C and D).

Figure 2. Raman spectra of TiO_2, TiO_2-Zn, TiO_2-Pd and TiO_2-Pd1.5%-Zn5%.

Figure 3. (A) XPS Cl 2p spectra of TiO2, TiO2-Pd, TiO2-Zn and TiO2-Pd-Zn; (B) Zn 2p and (C) Pd 3d spectra of TiO2-Pd and TiO2-Pd-Zn (TiO2-Pd1.5%-Zn5%).

Figure 4. (A) XPS valence band spectra, (B) absorption spectra, (C) surface photovoltaic spectra and (D) photoluminescence (PL) spectra of TiO_2, TiO_2-Zn, TiO_2-Pd and TiO_2-Pd1.5%-Zn5%.

Figure 5. CH_4 generation over TiO_2 (P25), TiO_2, TiO_2-Pd, TiO_2-Zn and TiO_2-Pd-Zn.

Figure 6. Schematic band structure of TiO2-PdX-ZnY as well as the photocatalytic mechanism (not drawn to scale).

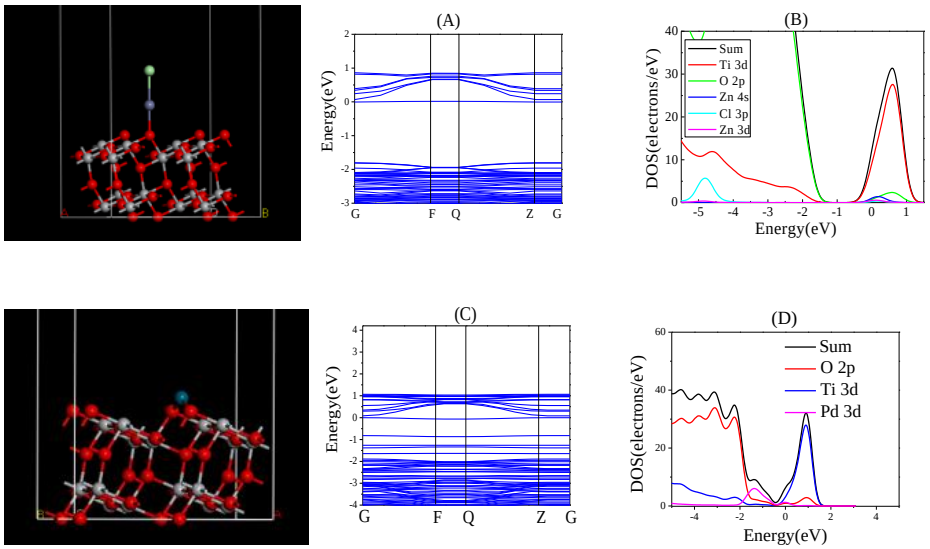

Figure 1. Theoretical calculated band structure and Projected density of states (PDOS) for the TiO_2-Zn (A and B) and TiO_2-Pd (C and D).

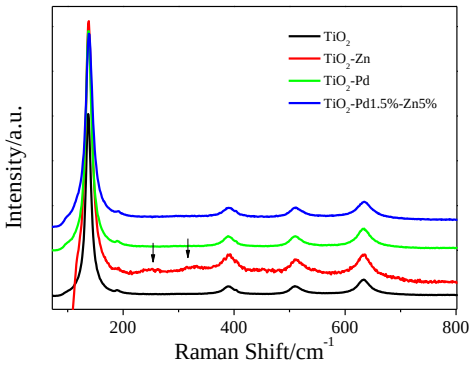

Figure 2. Raman spectra of TiO_2, TiO_2-Zn, TiO_2-Pd and TiO_2-Pd1.5%-Zn5%.

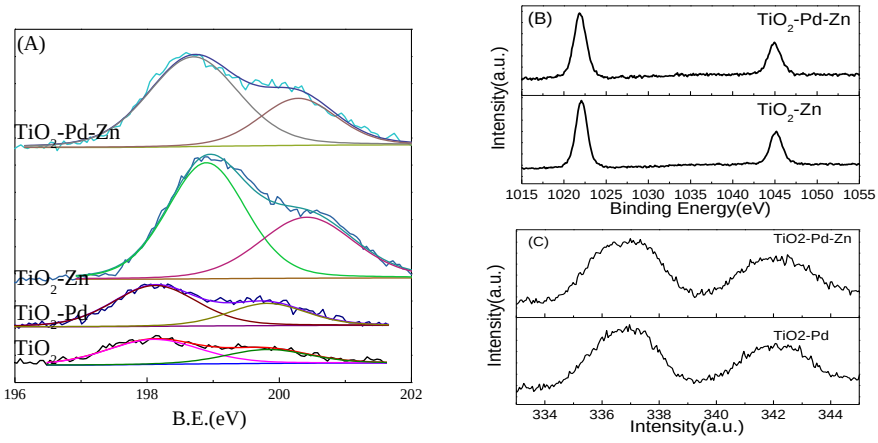

Figure 3. (A) XPS Cl 2p spectra of TiO2, TiO2-Pd, TiO2-Zn and TiO2-Pd-Zn; (B) Zn 2p and (C) Pd 3d spectra of TiO2-Pd and TiO2-Pd-Zn (TiO2-Pd1.5%-Zn5%).

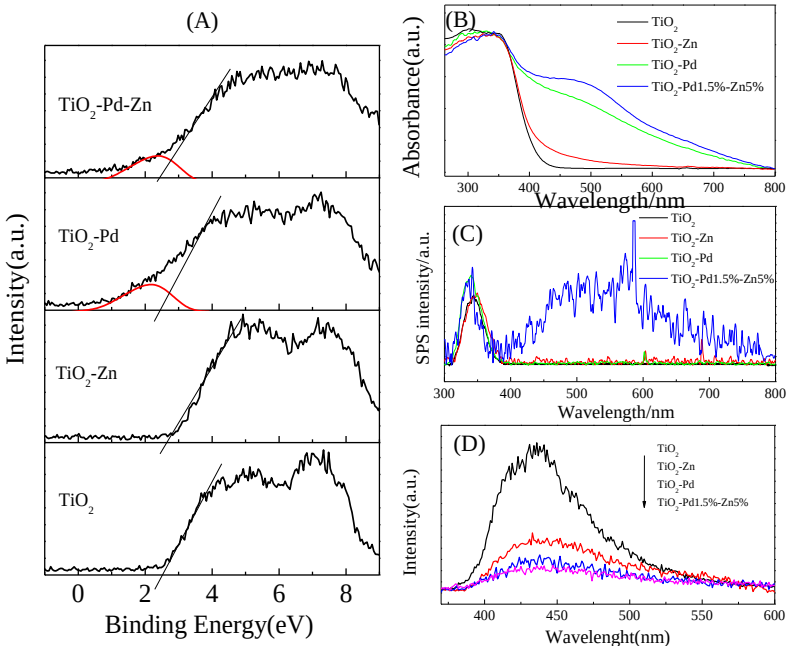

Figure 4. (A) XPS valence band spectra, (B) absorption spectra, (C) surface photovoltaic spectra and (D) photoluminescence (PL) spectra of TiO_2, TiO_2-Zn, TiO_2-Pd and TiO_2-Pd1.5%-Zn5%.

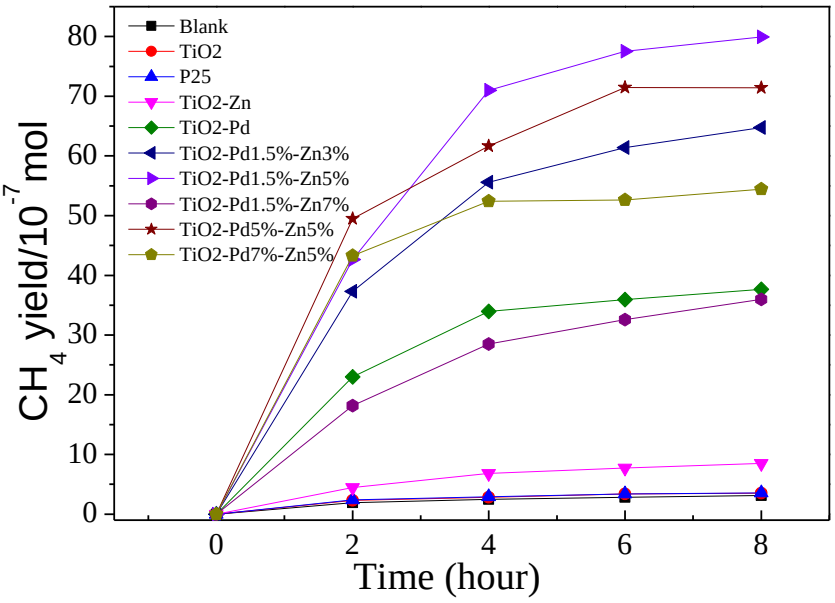

Figure 5. CH_4 generation over TiO_2 (P25), TiO_2, TiO_2-Pd, TiO_2-Zn and TiO_2-Pd-Zn.

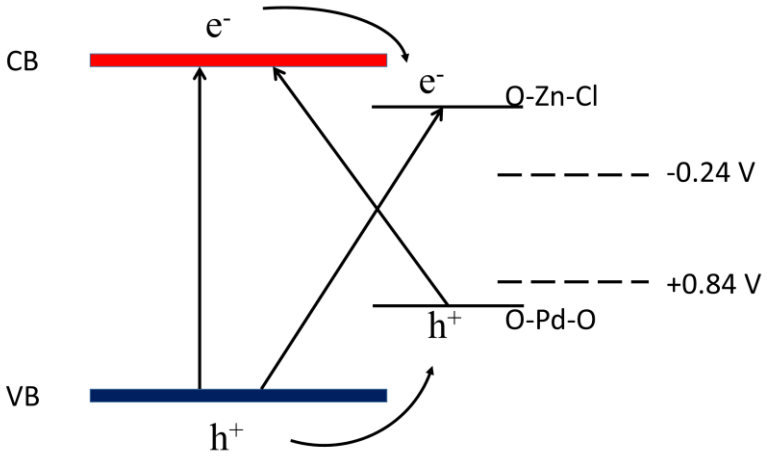

Figure 6. Schematic band structure of TiO2-PdX-ZnY as well as the photocatalytic mechanism (not drawn to scale).

Table 1.Values of Band Gap, Metal amount of Zn and Pd (Zn/Ti and Pd/Ti) from XPS, the Calculated Decay Time Constant τ1 and τ2 through Double Exponential Decay Fitting for the Corresponding Samples

	TiO_2	TiO_2-Zn	TiO_2-Pd	TiO_2-Pd1.5%-Zn5%
Band gap	3.10 eV	2.75 eV	2.50 eV	2.15 eV
Metal amount	0	Zn: 20.72%	Pd:3.34%	Zn: 25.43% Pd: 3.21 %
τ1(ns)	0.295	0.298	0.294	0.291
τ2(ns)	3.059	3.876	4.038	4.382

Table 2. Photocatalytic activity of pure TiO_2, TiO_2-Zn, TiO_2-Pd and TiO_2-PdX-ZnY samples under Xe lamp irradiation

Sample	CH4 generation amount (10-6mol)	specific photocatalytic activity [b] (10-6mol·g-1·h-1)
blank [a]	0.31±0.01	-
TiO2(P25)	0.36±0.02	0.30±0.02
TiO2	0.35±0.03	0.29±0.02
TiO2-Zn	0.85±0.02	0.71±0.02
TiO2-Pd	3.77±0.47	3.14±0.39
TiO2-Pd1.5%-Zn3%	6.48±0.27	5.40±0.23
TiO2-Pd1.5%-Zn5%	7.99±0.28	6.66±0.23
TiO2-Pd1.5%-Zn7%	3.60±0.35	3.00±0.29
TiO2-Pd5%-Zn5%	7.14±0.45	5.95±0.38
TiO2-Pd7%-Zn5%	5.44±0.73	4.53±0.61

[a]Blank is the photolysis of CO_2; [b]specific photocatalytic activity of CH_4, CH_4 generation amount per unit mass catalyst per hour

7: Electronic Supplementary Material

Click here to download 7: Electronic Supplementary Material: Supporting information.docx